



ACADEMIC
PRESS

Available online at www.sciencedirect.com

SCIENCE @ DIRECT®

Journal of Molecular Spectroscopy 221 (2003) 38–46

Journal of
MOLECULAR
SPECTROSCOPY

www.elsevier.com/locate/jms

The absorption spectrum of HDO around $1.0\ \mu\text{m}$ by ICLAS-VECSEL[☆]

Elena Bertseva,^a Olga Naumenko,^{a,b} and Alain Campargue^{a,*}

^a *Laboratoire de Spectrométrie Physique (associated with CNRS, UMR 5588), Université Joseph Fourier de Grenoble, B.P. 87, 38402 Saint-Martin-d'Hères, Cedex, France*

^b *Institute of Atmospheric Optics, Russian Academy of Sciences, Tomsk 634055, Russia*

Received 21 February 2003; in revised form 27 May 2003

Abstract

The HDO absorption spectrum has been recorded between 9625 and $10\,100\ \text{cm}^{-1}$ by intracavity laser absorption spectroscopy (ICLAS) based on a vertical external cavity surface emitting laser (VECSEL). Overall 1278 lines were attributed to the HDO species and were rovibrationally assigned using both the predictions based on the high-quality potential and dipole moment surfaces calculated by Schwenke and Partridge, and the spectrum simulation performed within the effective Hamiltonian approach. As a result, 289 precise energy levels were derived for the $(1\,0\,2)-(0\,2\,2)$ resonance dyad and 101 were assigned to the $(0\,3\,2)$, $(2\,3\,0)$, $(1\,5\,0)$, $(3\,1\,0)$, $(1\,1\,2)$, and $(0\,8\,0)$ states. The effective Hamiltonian modeling of the $(0\,2\,2)-(1\,0\,2)$ and $(1\,1\,2)-(0\,3\,2)$ interacting dyads is presented and discussed. A few local perturbations with highly excited bending levels could be identified.
© 2003 Elsevier Science (USA). All rights reserved.

1. Introduction

The study of the spectroscopic properties of water vapor and its isotopic species is of great importance for atmospheric science since water vapor represents the main absorber of the solar radiation. Great progress has been recently achieved in the theoretical calculations of water vapor line centers and intensities from high-quality ab initio potential and dipole moment surfaces [1,2]. This breakthrough in the theoretical understanding of the water vapor intramolecular dynamics stimulated new experimental studies of its high-resolution absorption spectra especially in the shortwave range (see, for instance, the recent review of [3]). Indeed, information about the rovibrational energy levels of the H_2^{16}O molecule derived from the spectra assignment has been significantly enlarged during the last five years [4]. Likewise, numerous new experimental data were ob-

tained on the rotational structure of the HDO vibrational states (see [5] and references therein). Still, as stressed in [5], progress for the HDO isotopomer has been much less satisfactory than for the H_2^{16}O species.

This new contribution is a part of our systematic intracavity laser absorption spectroscopy (ICLAS) investigation of the HDO absorption spectra up to $18\,500\ \text{cm}^{-1}$ [6–10]. In Fig. 1, we present an overview of the HDO spectrum as predicted by Schwenke and Partridge with the normal mode labeling and the corresponding reference of the experimental study, when available. Interestingly, nearly all the bands between 9500 and $18\,500\ \text{cm}^{-1}$, were investigated by ICLAS either with grating [6–10] or FT [11] detection. The $9161-9390\ \text{cm}^{-1}$ spectral region, which is just below the investigated region, was also previously studied by ICLAS-Nd glass and the corresponding $(1\,2\,1)-(0\,0\,0)$ and $(3\,1\,0)-(0\,0\,0)$ bands were rotationally assigned [12].

The whole above mentioned spectral region was also investigated by Fourier transform spectroscopy (FTS) with a $50\ \text{m}$ long cell located in Reims (France) but only the observation of the low rotational levels of the $6\nu_3$ and $7\nu_3$ overtones was reported so far [13].

[☆] Supplementary data for this article are available on ScienceDirect.

* Corresponding author. Fax: +04-76-51-45-44.

E-mail address: alain.campargue@ujf-grenoble.fr (A. Campargue).

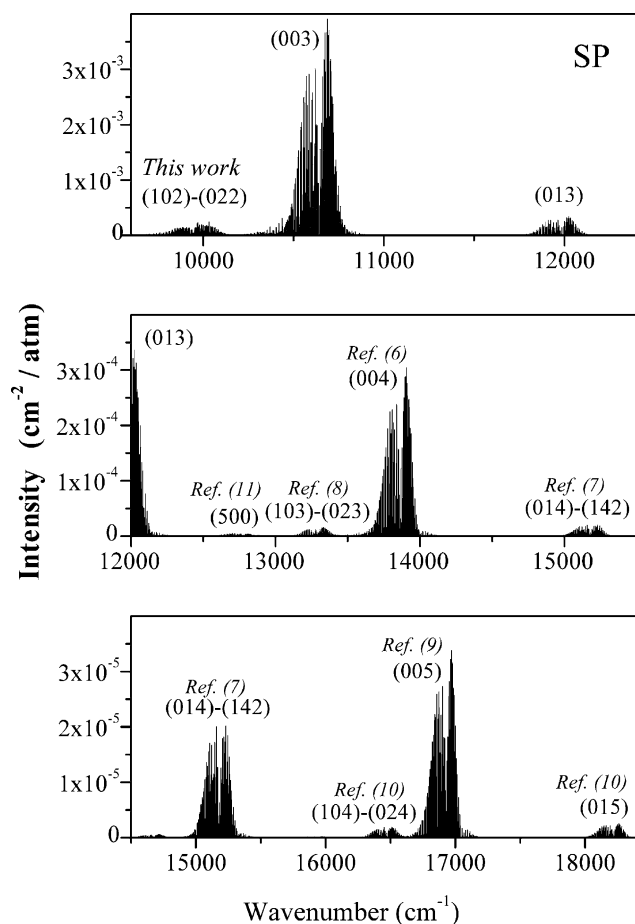


Fig. 1. Overview of the HDO spectrum as predicted by Schwenke and Partridge [1]. For each band, the normal mode labeling and the corresponding reference of the experimental study are given. Note the changes in the units of the intensity scale of the three sections.

The ICLAS spectrum presently recorded in the 9625–10 100 cm^{-1} spectral region is dominated by the $\nu_1 + 2\nu_3$ and $2\nu_2 + 2\nu_3$ bands (contrary to IUPAC recommendation, we use the traditional labeling of the vibrational modes: ν_1 (2723.68 cm^{-1}) is related to the OD stretching, ν_2 (1403.48 cm^{-1}) to the bending, and ν_3 (3707.47 cm^{-1}) to the OH stretching vibration). This spectral region was previously investigated by FTS [14] resulting in the derivation and successful modeling (using Watson-type A -reduced Hamiltonian) of the observed energy levels of the (1 0 2) and (0 2 2) interacting states. In the considered spectral region, 1278 lines observed in the ICLAS spectrum were attributed to the HDO isotopomer. The higher sensitivity provided by ICLAS allowed a doubling of the number of energy levels derived for these (1 0 2) and (0 2 2) states (289 compared to 149 in [14]), while about 100 experimental energy levels were derived for the first time and assigned to six other vibrational states: (0 3 2), (1 1 2), (1 5 0), (2 3 0), (3 1 0), and (0 8 0). As described below, the rovibrational assignments rely both on the comparison with Schwenke and Partridge (SP)

Table 1
Summary of the experimental information relative to the bands of HDO analyzed by ICLAS between 9625 and 10 100 cm^{-1}

Band	$E_{[000]}^a$		Number of observed levels
	Ref. [1]	Obs.	
3 1 0–0 0 0	9293.025		23
1 5 0–0 0 0	9381.590		17
2 3 0–0 0 0	9488.133		14
0 2 2–0 0 0	9934.815	9934.789	149
1 0 2–0 0 0	9967.107	9967.023	140
0 8 0–0 0 0	10119.367		1
0 3 2–0 1 0	11243.060	11242.923	35
1 1 2–0 1 0	11315.433	11315.415 ^b	11

^a Vibrational energy level of the upper state (cm^{-1}).

^b Fitted value obtained from a limited number of levels (cm^{-1}).

database [1,2] and on the calculations within the effective Hamiltonian approach. The list of the vibrational transitions relevant for the present study is presented in Table 1.

2. Experimental details

The ICLAS spectra were recorded with the experimental setup based on a vertical external cavity surface emitting laser (VECSEL), previously described in [15–17] and applied recently to the spectroscopy of CO_2 [18], N_2O [17,19], H_2S [20], and OCS [21]. Quantum well semiconductor structures have been used as amplifying media giving access to the 8800–10 100 cm^{-1} region, not accessible by ICLAS-Ti:Sapphire. The intracavity cell containing the absorber is inserted in the long arm of the external cavity as described in [15–17]. A detailed description of the spectrometer can be found in the original papers of Garnache et al. [15,16]. Two structures made of InGaAs based semiconductors, allowed for a continuous coverage of the 9625–10 100 cm^{-1} spectral region. The spectra were recorded with generation times up to 270 μs , leading to equivalent absorption path lengths up to 35 km. The intracavity sample cell was filled with a 1:1 mixture of H_2O and D_2O at a pressure of 20 Torr (26.3 hPa) just below the vapor pressure at room temperature (25 $^\circ\text{C}$). This procedure is assumed to lead to a mixture of $\text{H}_2\text{O}:\text{HDO}:\text{D}_2\text{O}$ in the proportion 1:2:1. Two examples of spectra are presented in Figs. 2 and 3, respectively.

The region simultaneously recorded with a 3724 diodes silicon array is about 12 cm^{-1} according to the dispersion of our grating spectrograph. Each 12 cm^{-1} window was calibrated separately with the help of well-calibrated lines appearing in the spectrum. These reference lines were either strong HDO lines previously measured by FTS [14], lines due to H_2O present in the cell [22], or C_2H_2 lines [23] added as trace in the cell in the 9625–9690 cm^{-1} region, where no reliable reference

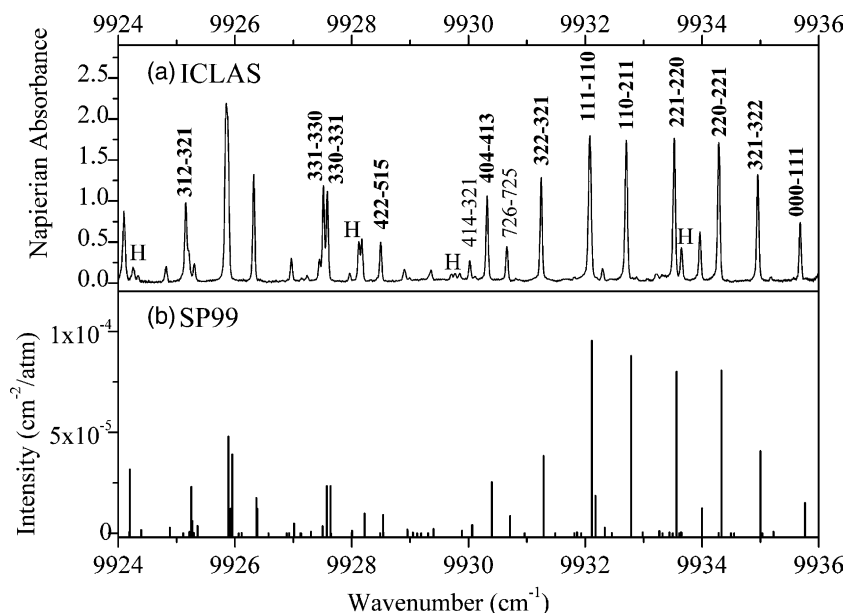


Fig. 2. The HDO absorption spectrum in the 9924–9936 cm^{-1} spectral region close to the origin of the (022)–(000) band. The $J'K'_aK'_c - J''K''_aK''_c$ rotational assignments are given for part of the lines (the whole assignments are listed in the supplement material). The rotational assignments written in bold characters are related to the (102) vibrational state while the others correspond to the (022) vibrational state. “H” marks the most intense lines due to H_2^{16}O . (a) ICLAS-VECSEL spectrum recorded with an equivalent path length of about 22 km and a total vapor pressure of 4 Torr. (b) HDO spectrum calculated by Schwenke and Partridge from ab initio potential energy and dipole moment surfaces [1,2].

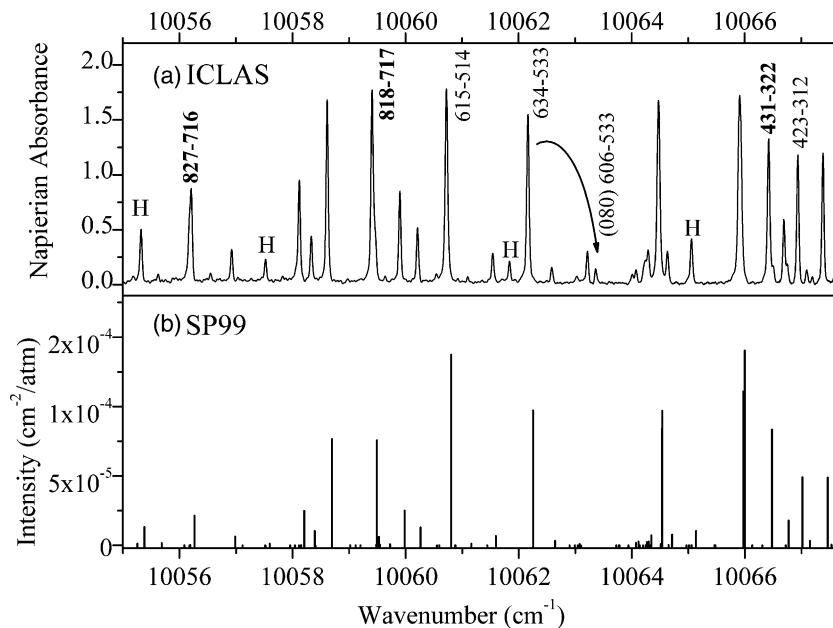


Fig. 3. Same as Fig. 2 for the 10055–10066 cm^{-1} spectral region. The ICLAS-VECSEL spectrum was recorded with an equivalent path length of about 10.5 km and a total vapor pressure of 6 Torr. Note the strong local interaction between the (022) [634] level at 10435.824 cm^{-1} and the (080) [606] level at 10438.18 cm^{-1} which induces a significant intensity transfer to the transition observed at 10063.362 cm^{-1} reaching the (080) [606] energy level.

lines of water were found. From the comparison of the wavenumber values obtained using independent reference lines, the accuracy of the ICLAS line positions is estimated to be around 0.005 cm^{-1} .

3. Results and discussion

For identification purpose, rough intensities were derived for each observed line from the peak absorption.

The SP HDO database [1,2] was used as a guide in the spectrum assignment. As showed by the comparison included in Figs. 2 and 3, the identification of the strongest (102)–(000) and (022)–(000) bands was straightforward provided that the line positions were predicted by SP within 0.16 cm^{-1} , and that the observed line positions allowed for well-defined combination differences. Overall 140 and 149 energy levels were derived for the (102) and (022) upper states, respectively, by adding the ground state experimental energy levels [24] to the observed transitions (see Table 2).

At the second step, we assigned weaker transitions which were found to belong to six additional vibrational states. The most complete energy levels set of these six states (35 rotational levels) was derived for the (032) state at 11242.923 cm^{-1} , from the hot transitions originating from the (010) rotational sublevels (taken from [24]), while only 11 energy levels of the (112) state at 11315.415 cm^{-1} [1] were obtained from the (112)–(010) hot band. For the other four weak cold bands (see Table 1), we observed only separate highly excited *R* lines not included into combination differences that hindered unambiguous assignment. In this case, we relied only on SP calculations for the assignment. Though the deviations of the observed line positions from SP predictions reach 0.4 cm^{-1} (see below) for the (310)–(000) band, they are nearly constant for each identified band with slow variations as *J* increases. This evolution combined with the line intensities control was sufficient for a confident assignment of the discussed transitions. Finally we could identify 96% of the observed HDO lines. The resulting linelist of 1468 transitions is attached as supplementary material. In this list the experimental frequencies are listed followed by the SP intensities [2] and rovibrational assignment. The vibrational energies and number of derived energy levels for all observed states are summarized in Table 1 together with a comparison with the predictions of [1].

After the spectrum identification, we attempted the energy levels fitting for the (102)–(022) and (032)–(112) dyads. Since the HDO molecule undergoes strong centrifugal distortion, we used the effective rotational Hamiltonian written through Padê–Borel approximants [25,26]. This approach is attractive for two reasons: first, it improves the convergence of perturbation series, which represent the matrix elements of effective Hamiltonian; second, comparison of the retrieved parameters values is possible as it leads to rotational constants close to those obtained with the Watson-type rotational Hamiltonian.

As stressed in [14], the (102) and (022) states strongly interact both through Fermi- and Coriolis-type interactions. In the vibrationally nondiagonal blocks, we used the resonance operators in the form

$$H_{vv'} = C_y(iJ_y) + C_{xz}\{J_x, J_z\} + \dots \quad (1)$$

for Coriolis-type resonance, and

$$H_{vv'} = F_0 + F_k J_z^2 + F_j J^2 + F_{xy} J_{xy}^2 + F_{xyj} J^2 J_{xy}^2 + \dots \quad (2)$$

for Fermi-type resonance, with $\{A, B\} = AB + BA$ and $J_{xy}^2 = J_x^2 - J_y^2$.

At the first step, we tried to reproduce our set of energy levels using the parameters of [14], but we obtained large deviations (up to several cm^{-1}) for high *J* and K_a levels not observed by FTS [14]. This confirms the fact that the Watson-type Hamiltonian, though allowing for a rather good fitting, has poor predictive ability for nonrigid molecules. Then, we preferred a different choice of initial parameters and another type of rotational operator. As initial approximation, we took the parameters set obtained for the (101)–(021) dyad [27]. In this case we could check the consistency of our fitted centrifugal distortion parameters which are expected to remain close to their initial values. Note that constraining the high-order centrifugal distortion parameters to their ground state values (as assumed in [14]) is not justified, at least for the (022) state which is affected by strong centrifugal distortion effect.

Among the 289 energy levels of the dyad, 269 could be reproduced with an rms of 0.008 cm^{-1} , that is slightly larger than the experimental accuracy (0.0032 cm^{-1} estimated for the levels determined from several transitions), by varying 31 parameters (in [14], 33 varied parameters were needed to fit 149 energy levels within 0.005 cm^{-1}). About 20 energy levels were found perturbed by local resonances with some dark states and were then excluded from the fit. The experimental energy levels for the (102)–(022) states are presented in Table 2, while the corresponding parameters are listed in Table 3.

Our analysis showed that the vibrational coupling constant, F_0 , should be considered. In general, the relevance of this parameter in the fit process depends on the vibrational states and on the molecules. Sometimes, it is fixed to zero since it is strongly correlated with the vibrational energies, E_v , that complicates the fitting. But in our case, the F_0 parameter was found to be required and well defined like in the case of the (101)–(021) [29,30], and (100)–(020) [28] dyads. The obtained value of F_0 (15.5 cm^{-1}) is larger than the energy separation of the zero energy levels of the interacting states (9.0 cm^{-1}) leading to a strong anharmonic mixing. Table 3 shows that the obtained parameters values are consistent and do not show unexpected changes in sign and amplitude in particular for the distortion constants.

Our vibrational assignments for the (102)–(022) states coincide mostly with those of SP [1]. It is interesting to note that we detected a strong local interaction between the (022) [634] level at 10435.824 cm^{-1} and the (080) [606] level at 10438.18 cm^{-1} [1]. This interaction shifts the (022) [634] level by only 0.05 cm^{-1} , but induces a significant intensity transfer to transitions

Table 2
Observed energy levels for the (0 2 2), (1 0 2), (1 1 2), and (0 3 2) vibrational states of HDO

J	K _a	K _c	(022)			(102)				(032)				(112)			
			E _{obs}	σ	N	o – c	E _{obs}	σ	N	o – c	E _{obs}	σ	N	o – c	E _{obs}	N	o – c
0	0	0	9934.789	13	2	1	9967.023	1	2	-3	11242.923		1	13			
1	0	1	9950.065	8	3	-10	9982.239	2	3	-8	11258.346	3	2	13			
1	1	1	9964.567	1	3	-7	9995.908	3	3	-8							
1	1	0	9967.635	2	3	9	9998.880	2	3	-5	11279.734		1	-34			
2	0	2	9980.184	4	4	-10	10012.250	7	5	-7	11288.739	1	2	13	11360.588	1	-9
2	1	2	9992.024	2	6	-11	10023.422	4	5	1	11303.737		1	-34	11372.578	1	-11
2	1	1	10001.170	3	4	7	10032.330	2	6	-5	11313.951		1	-28			
2	2	1	10074.711	1	5	-3	10042.786	2	4	-1							
2	2	0	10075.146	5	5	-3	10043.210	3	5	2	11367.001	4	2	23	11426.392	1	13
3	0	3	10024.305	6	6	1	10056.254	3	5	-1	11333.250	2	2	11			
3	1	3	10032.950	4	8	-11	10064.423	4	8	1	11344.603	2	3	-15			
3	1	2	10051.101	5	7	6	10082.227	2	6	2	11364.961		1	6			
3	2	2	10120.637	2	6	5	10088.303	4	8	-3	11412.640	4	2	12	11471.629	1	-1
3	2	1	10122.757	2	7	4	10090.336	2	6	-3	11415.058	1	2	-23			
3	3	1	10202.146	9	3	2	10160.568	5	5	6				11503.428	1	-10	
3	3	0	10202.172	3	3	-11	10160.605	2	6	4							
4	0	4	10081.412	3	6	3	10113.299	5	7	2	11390.832	2	2	6			
4	1	4	10087.083	4	7	-2	10118.665	3	7	2	11398.624		1	-6			
4	1	3	10116.936	3	6	10	10147.724	2	7	7	11432.263		1	27			
4	2	3	10181.514	2	6	1	10149.063	5	8	-8				11532.192	1	-9	
4	2	2	10187.540	2	8	7	10154.357	5	0	0	11479.879		1	33			
4	3	2	10264.380	2	4	-4	10221.540	4	5	-1							
4	3	1	10264.655	7	3	1	10221.806	3	8	-2							
4	4	1	10379.056	6	3	-7	10316.900	6	4	3	11739.600		1	3			
4	4	0	10379.064	1	2	-1	10316.912	4	3	11	11739.598		1	-2			
5	0	5	10150.741	2	8	3	10182.658	3	7	5							
5	1	5	10154.126	3	4	-3	10185.869	3	7	-2	11465.523	1	2	10	11534.058	1	-26
5	1	4	10229.856	6	3	1	10197.943	2	9	13	11515.150		1	7			
5	2	4	10257.078	5	7	11	10223.124	4	8	-1	11549.348		1	-41	11607.382	1	11
5	2	3	10269.951	2	5	10	10235.586	2	8	5	11562.525		1	43			
5	3	3	10342.302	7	4	-15	10297.844	3	5	-3				11642.629	1	9	
5	3	2	10343.368	1	4	2	10298.880	3	6	-2							
5	4	2	10456.915	6	3	3	10392.796	3	4	6							
5	4	1	10456.944	1	2	7	10392.819	2	3	2							
5	5	1	10602.669	6	3	6	10512.099	4	3	-3							
5	5	0	10602.669	6	3	6	10512.106	5	4	4							
6	0	6	10231.960	3	9	7	10263.998	3	6	2	11542.105	2	2	-3			
6	1	6	10233.842	2	8	1	10265.799	2	7	3	11545.028	1	2	31			
6	1	5	10325.955	4	4	7	10293.150	6	7	9	11612.735		1	-9			
6	2	5	10346.954	2	6	3	10311.936	2	6	-5	*11639.292	9	2	-100			
6	2	4	10369.909	5	5	1	10333.798	3	7	-1	11662.743		1	-4			
6	3	4	*10435.824	5	4	-54	10389.395	2	6	-4				*11735.026	1	-485	
6	3	3	10438.879	6	5	2	10392.337	2	8	-4							
6	4	3	10550.531	5	3	-1	10484.045	2	5	2							
6	4	2	10550.648	3	4	-7	10484.179	2	5	6							
6	5	2	10695.875	2	3	-1	10602.800		1	0							
6	5	1	10695.878	1	3	-1	10602.805		1	3							
6	6	1	10870.124	5	2	6	10745.969		1	-15							
6	6	0	10870.124	5	2	6	10745.970		1	-13							
7	0	7	10325.022	2	6	4	10357.285	2	5	4	11635.213	3	2	-20			
7	1	7	10326.018	3	6	-1	10358.232	8	5	-9	11636.891		1	37			
7	1	6	10435.687	2	4	7	10401.464	3	6	7							
7	2	6	10450.786	4	4	7	10414.397	3	5	-9	*11743.065		1	-208	11800.101	1	-18
7	2	5	10486.891	3	5	-2	10448.379	2	3	-3	11780.050	9	2	-28			
7	3	5	10544.920	4	4	27	10496.042	2	6	-6							
7	3	4	10551.852	2	3	-1	10502.774	1	3	-3							
7	4	4	10659.970	2	4	-8	10590.707	1	3	1							
7	4	3	10660.405	2	4	-14	10591.172	3	3	4							
7	5	3	10804.770	6	3	4	10708.763	2	2	3							
7	5	2	10804.780	9	3	2	10708.761		1	-13							
7	6	2	10978.522	3	3	-7	10851.364	3	2	-13							

Table 2 (continued)

<i>J</i>	<i>K_a</i>	<i>K_c</i>	(0 2 2)				(1 0 2)				(0 3 2)				(1 1 2)		
			<i>E_{obs}</i>	<i>σ</i>	<i>N</i>	<i>o - c</i>	<i>E_{obs}</i>	<i>σ</i>	<i>N</i>	<i>o - c</i>	<i>E_{obs}</i>	<i>σ</i>	<i>N</i>	<i>o - c</i>	<i>E_{obs}</i>	<i>N</i>	<i>o - c</i>
7	6	1	10978.522	3	3	-7	10851.367	1	2	-9							
7	7	1	11179.007	2	3	-6	11017.802		1	12							
7	7	0	11179.007	2	3	-6	11017.802		1	12							
8	0	8	10430.009	3	4	3	10462.570	1	3	7	11740.001		1	-32			
8	1	8	10430.525	6	5	5	10463.062	2	5	4	*11740.997	5	2	82			
8	1	7	10558.040	1	3	-2	10521.901	4	8	2							
8	2	7	10568.141	3	5	-9	10530.136	5	7	-5							
8	2	6	10620.779	6	3	1	10578.455	2	4	-4							
8	3	6	10669.088	6	4	10	10616.812	2	4	-17							
8	3	5	10682.817	2	5	-1	10630.607	4	5	0							
8	4	5	10785.257	2	3	-7	10712.791	3	3	6							
8	4	4	10786.541	4	5	15	10714.116	1	3	5							
8	5	4	10929.381		1	-6	10830.044	1	2	2							
8	5	3	10929.432		1	-5	10830.114	3	2	15							
8	6	3	11102.506	2	2	3	10971.917	1	2	-6							
8	6	2	11102.507	4	2	3	10971.918		1	-6							
8	7	2	11302.443		1	-3											
8	7	1	11302.443		1	-3											
8	8	1	11527.141	1	2	2											
8	8	0	11527.141	1	2	2											
9	0	9	10546.988	2	4	5	10579.898	4	4	6	11856.590	5	2	5			
9	1	9	10547.239	3	5	-1	10580.140	2	3	-1	*11857.248		1	192			
9	1	8	10692.325	1	3	-10	10653.886	2	5	-1							
9	2	8	10698.673	2	5	-12	10658.774	2	6	-10							
9	2	7	*10769.076		1	-39	10722.993	2	3	-6							
9	3	7	10808.060	4	4	6	10752.796	3	5	-11							
9	3	6	10831.863	6	3	-10	10775.803	5	5	2							
9	4	6	10926.314	5	3	-6	10850.235	2	3	8							
9	4	5	10929.405	3	2	1	10853.451	1	3	8							
9	5	5	11069.797	1	2	12	10966.711	2	3	9							
9	5	4	11069.954	5	2	-2	10966.903	1	2	10							
9	6	4	11242.078	4	2	13	11107.665		1	4							
9	6	3	11242.076	3	2	6	11107.665		1	-2							
9	7	3	11441.321		1	2											
9	7	2	11441.321		1	1											
10	0	10	10675.992	2	4	6	10709.308	6	4	11							
10	1	10	10676.115	2	4	3	10709.423	2	4	3							
10	1	9	10838.245	1	4	-18	10797.274	2	5	0							
10	2	9	10842.039	6	2	-11	10800.022	2	5	-10							
10	2	8	*10931.700	2	2	-113	10880.864	1	4	-2							
10	3	8	10961.380	6	3	0	10902.463	3	3	-6							
10	3	7	10998.321		1	7	10937.826	2	3	-6							
10	4	7	11082.982	1	2	0	11003.143	1	2	5							
10	4	6	11089.584		1	-5	11009.704	1	2	5							
10	5	6	11225.986		1	2	11118.776		1	0							
10	5	5	11226.464	1	2	-9	11119.336	4	2	13							
10	6	5	*11397.292		1	52	11258.641		1	6							
10	6	4	*11397.326		1	67	11258.641		1	-16							
11	0	11	10817.039	1	2	13	10850.779	6	2	0							
11	1	11	10817.090	6	3	3	10850.832	4	3	-6							
11	1	10	10995.790	7	3	-12	10952.159	3	5	0							
11	2	10	10997.966	2	2	-7	10953.650	1	4	-1							
11	2	9	*11107.459	5	3	36	11050.976	1	3	2							
11	3	9	11128.594	2	4	7	11065.609		1	-5							
11	3	8	11182.565	9	2	-14	11115.826		1	0							
11	4	8	11254.990	2	2	15	11169.975	2	2	8							
11	4	7	11267.588		1	5	11183.344		1	-1							
11	5	7	11397.957		1	-7	11286.265	1	2	-10							
11	5	6					11287.639		1	6							
12	0	12	10970.105	2	2	9	11004.318	4	3	-6							
12	1	12	10970.118		1	-6	11004.347	3	3	-5							
12	1	11	11165.017	7	2	-25	11118.675	4	5	-10							

Table 2 (continued)

<i>J</i>	<i>K_a</i>	<i>K_c</i>	(0 2 2)				(1 0 2)				(0 3 2)				(1 1 2)		
			<i>E_{obs}</i>	σ	<i>N</i>	o – c	<i>E_{obs}</i>	σ	<i>N</i>	o – c	<i>E_{obs}</i>	σ	<i>N</i>	o – c	<i>E_{obs}</i>	<i>N</i>	o – c
12	2	11	11166.263	3	2	16	11119.469	3	4	0							
12	2	10	*11294.849	1	2	–55	11232.528	3	2	8							
12	3	10	11309.221		1	18	11241.824		1	–11							
12	3	9	11381.884		1	8	11308.720		1	15							
12	4	9	*11441.983		1	57	11352.047	2	2	7							
12	4	8	*11463.486		1	89	11374.502		1	–19							
12	5	8	11585.619		1	–14											
12	5	7	*11588.302		1	–80	11472.175		1	–7							
13	0	13	11135.183		1	6	11169.931	1	2	8							
13	1	13	11135.188	7	2	–2	11169.919	2	2	8							
13	1	12	*11346.307	1	2	235	11296.956	1	2	–7							
13	2	12	*11346.981	1	2	259	11297.367	6	3	–1							
13	2	11	*11493.285		1	–342	11425.160		1	17							
13	3	11	11502.799		1	–2	11430.756	5	2	–7							
13	3	10	*11596.313		1	575	11515.273	2	2	–3							
13	4	10	*11643.536		1	145											
13	5	8	*11793.235		1	–1093											
14	0	14	*11312.173		1	–72	11347.508	4	3	–1							
14	1	14	11312.226	2	2	–23	11347.521	10	2	7							
14	1	13	*11538.829		1	–121	11487.055		1	–3							
14	2	13	11539.296		1	7	11487.281		1	19							
14	3	12					11632.088		1	1							
15	0	15	11501.255	2	2	–13	*11537.035		1	–51							
15	1	15	11501.263	6	2	–7	11537.075		1	–12							
15	1	14	11743.704		1	3	11688.994		1	5							
15	2	14					11689.084		1	–7							
16	0	16	11702.226		1	12											
16	1	16	11702.220		1	7											
16	2	15	*11960.635		1	232											

Notes. Asterisks mark the energy levels excluded from the fit. (o – c) are observed minus computed (EH) energy levels values in 10^{-3} cm^{-1} . σ denotes the experimental uncertainties of the levels given in 10^{-3} cm^{-1} . *N* is the number of lines sharing the same upper level. (Note that for the (1 1 2) state, all levels were derived from a single line.)

reaching the (0 8 0) [6 0 6] energy level (see Fig. 3). This last level was derived from two rather strong lines deviating by -1.15 cm^{-1} from the SP predicted centers (see Table 5). Local interactions of the (0 2 2) state with unidentified highly excited dark states become stronger and stronger as *J* increases: from the nine observed levels with *J* = 13, six were found affected by strong perturbations and excluded from the fit.

Let us now consider the second dyad of strongly interacting (0 3 2)–(1 1 2) vibrational states. Using the more or less complete set of the low *J* energy levels of the (0 3 2) state, we attempted to apply the EH approach to this system. Since we have a limited set of input data, we carefully prepared the initial set of data using all available information: (i) all the centrifugal distortion constants of the (1 1 2) and (0 3 2) states were fixed to the corresponding values of the (2 1 0) [27] and (0 2 2) (Table 3) states, respectively, and (ii) the band center and rotational constants were estimated from the fitting of the low *J* levels of [1]. Thus, by varying 10 parameters, we could reproduce with an rms of 0.024 cm^{-1} , 41 of the 46 energy initially introduced into the fit. This rather large value of the rms shows that perturbations with other dark states play probably a role. The set of observed energy levels for the (0 3 2) and

Table 3
Rotational, centrifugal distortion, and coupling constants of the (0 2 2) and (1 0 2) vibrational states of HD¹⁶O (cm^{-1})

	(0 2 2)	(1 0 2)
<i>E_v</i>	9946.4180(1 5 0)	9955.3957(1 5 0)
<i>A</i>	25.35950(1 5 0)	21.125023(8 6 0)
<i>B</i>	9.373424(4 0 0)	8.906132(3 6 0)
<i>C</i>	6.078680(2 1 0)	6.149812(2 2 0)
<i>Δ_k</i>	$3.6223(1 1 0) \times 10^{-2}$	$9.7997(1 5 0) \times 10^{-3}$
<i>Δ_{jk}</i>	$-2.219(2 3 0) \times 10^{-4}$	$1.0476(2 0 0) \times 10^{-3}$
<i>Δ_j</i>	$4.8551(1 3 0) \times 10^{-4}$	$3.7644(1 1 0) \times 10^{-4}$
<i>δ_k</i>	$5.4677(1 2 0) \times 10^{-3}$	$2.13711(9 3 0) \times 10^{-3}$
<i>δ_j</i>	$1.82080(5 9 0) \times 10^{-4}$	$1.33358(9 3 0) \times 10^{-4}$
<i>H_k</i>	$3.3864(4 7 0) \times 10^{-4}$	4.44×10^{-5}
<i>H_{kj}</i>	$-5.1132(7 0 0) \times 10^{-5}$	$-9.746(3 5 0) \times 10^{-6}$
<i>H_{jk}</i>	$7.107(1 1 0) \times 10^{-6}$	$2.3905(9 6 0) \times 10^{-6}$
<i>H_j</i>		7.45×10^{-8}
<i>h_k</i>	1.72×10^{-4}	2.15×10^{-5}
<i>h_{kj}</i>		2.26×10^{-6}
<i>h_j</i>		$2.924(3 5 0) \times 10^{-8}$
<i>L_k</i>	$-4.322(2 3 0) \times 10^{-7}$	-1.15×10^{-7}
Coupling parameters		
<i>F₀</i>		15.48137(3 6 0)
<i>F_k</i>		$-1.894(1 9 0) \times 10^{-2}$
<i>F_j</i>		$9.1820(5 6 0) \times 10^{-3}$
<i>F_{xyj}</i>		$4.845(2 6 0) \times 10^{-6}$
<i>C_y</i>		0.28760(2 3 0)
<i>C_{xz}</i>		$-3.994(6 5 0) \times 10^{-3}$

Table 4
Rotational, centrifugal distortion, and coupling constants of the (1 1 2) and (0 3 2) vibrational states of HD¹⁶O (cm⁻¹)

	(1 1 2)	(0 3 2)
E_v	11300.9020(9 5 0)	11257.4228(9 9 0)
A	22.81860(6 3 0)	28.42245(9 4 0)
B	9.041	9.53192(1 0 0)
C	6.088	5.971773(7 6 0)
Δ_k	2.10×10^{-2}	$6.5383(5 9 0) \times 10^{-2}$
Δ_{jk}	1.03×10^{-3}	-2.22×10^{-4}
Δ_j	3.38×10^{-4}	4.86×10^{-4}
δ_k	3.53×10^{-3}	5.47×10^{-3}
δ_j	1.28×10^{-4}	1.82×10^{-4}
H_k	1.86×10^{-4}	3.39×10^{-4}
<i>Coupling parameters</i>		
F_0	29.0110(7 5 0)	
F_k	-0.3303(1 0 0)	
C_v	0.5792(2 3 6)	

(1 1 2) states is included in Table 2 while the parameters set is presented in Table 4.

The remaining 54 energy levels (Table 5) not considered in the fitting process were derived from separate transitions reaching the (1 5 0), (2 3 0), and (3 1 0) states. The EH description of these levels cannot be applied because of the lack of sufficient experimental information. In consequence, we relied only on SP calculation in the assignment of the corresponding transitions. The deviation from SP predictions included in Table 5, are relatively

large but their regular variation confirms the correctness of the assignments. SP rovibrational assignments are sometimes ambiguous and then require a checking. In order to check the SP assignments for the (1 5 0), (2 3 0), and (3 1 0) states, we intended to reproduce the predicted [1] energy levels within EH approach considering these states as isolated. In the case of the (3 1 0) state, strong local resonance with the (0 7 0) state for the $K_a = 2$ energy levels was evidenced, but the other energy levels can be roughly reproduced in the isolated scheme confirming the reliability of SP assignments for the (3 1 0) state.

The SP energy levels set attributed to the (2 3 0) state looks more “suspicious:” despite the high-bending excitation, the energy of the levels is not predicted to increase with K_a . However, in the case of the (2 3 0) and also of the (1 5 0) states, we failed to reassign the SP identification. The ambiguity of SP assignments are due to the strong resonance mixing between the (1 5 0), (2 3 0), and (0 7 0) states, the last one being also strongly connected with the (1 2 1) state. Finally, considering this situation we decided to adopt the SP assignments for the (1 5 0) and (2 3 0) states (Table 5). More experimental information is then needed to fix this problem.

For completeness, we mention that the linelist of the supplementary material includes 3 lines assigned to the (4 0 0) upper state at 10378.64 cm⁻¹ which could be identified.

Table 5
Observed energy levels for the (2 3 0), (1 5 0), and (3 1 0) vibrational states of HDO (cm⁻¹)

(2 3 0)					(1 5 0)					(3 1 0)				
J	K_a	K_c	E_{obs}	Δ	J	K_a	K_c	E_{obs}	Δ	J	K_a	K_c	E_{obs}	Δ
4	4	1	9928.667	0.05	5	2	3	9838.979	-0.24	8	7	2	10612.776	-0.27
4	4	0	9928.640	0.02	5	3	3	9984.153	-0.22	8	7	1	10612.776	-0.27
5	3	3	9874.799	0.02	5	3	2	9984.467	-0.22	8	8	1	10842.907	-0.32
5	3	2	9875.237	0.02	6	2	4	9937.998	-0.23	8	8	0	10842.907	-0.32
5	4	2	10004.299	0.04	6	3	4	10078.600	-0.22	9	7	3	10743.574	-0.26
5	4	1	10004.305	0.04	7	2	6	10028.067	-0.19	9	7	2	10743.573	-0.26
6	3	4	9967.805	0.02	7	2	5	10054.540	-0.22	9	8	2	10972.898	-0.32
6	3	3	9969.055	0.01	7	3	5	10188.712	-0.24	9	8	1	10972.898	-0.32
6	4	3	10095.218	0.04	7	3	4	10190.958	-0.21	9	9	1	11228.627	-0.39
6	4	2	10095.267	0.04	8	1	7	10107.709	-0.18	9	9	0	11228.627	-0.39
6	5	2	10285.612	0.07	8	2	7	10148.130	-0.18	10	9	2	11372.115	-0.39
6	5	1	10285.596	0.06	8	2	6	10188.256	-0.22	10	9	1	11372.115	-0.39
7	3	4	10079.264	0.02	9	1	8	10248.530	-0.18	11	8	4	11276.210	-0.32
7	4	4	10201.484	0.05	9	2	7	10338.051	-0.20	11	8	3	11276.210	-0.32
8	3	5	10206.176	0.03	10	1	9	10402.086	-0.15					
8	4	5	10323.145	0.07	10	2	9	10430.324	-0.19					
9	3	7	10339.784	0.00	14	2	12	11312.545	-0.13					
9	3	6	10349.960	0.00										
9	4	6	10460.053	0.05										
9	4	5	10461.421	0.06										
10	3	7	10510.688	0.04										
10	4	7	10612.424	0.06										
11	4	8	10780.013	0.07										
(0 8 0)														
6	0	6	10437.029	-1.15										

Notes. Δ (cm⁻¹) is the difference between the experimental energy levels and SP predictions [1]. Most of the levels presented in this table, were derived from a single line.

4. Conclusion

The high-resolution absorption spectrum of HDO has been recorded and theoretically treated in the 9625–10 100 cm^{-1} spectral range. The high sensitivity provided by ICLAS has allowed the doubling of the number of the observed energy levels of the (1 0 2) and (0 2 2) states, previously determined from FT measurements [14] and the new determination of about 100 energy levels which were attributed to the highly excited (1 5 0), (3 1 0), (2 3 0), (0 3 2), and (1 1 2) states. About 80% of the 390 observed energy levels could be assigned and modeled in the frame of the effective Hamiltonian approach with the average accuracy close to the experimental one, confirming in most cases the SP assignments. However, the lack of experimental information relative to the (2 3 0) and (1 5 0) states prevents applying the EH approach and then the checking rovibrational assignments proposed in [1]. The excellent overall agreement between our measurements and SP predictions [1] observed up to 18 500 cm^{-1} in our previous contributions, is fully confirmed around 1 μm .

Strong resonance perturbations with dark states were evidenced for the (0 2 2) state, resulting in particular in the observation of two transitions reaching the (0 8 0) highly excited bending state. SP rovibrational assignments of the transitions reaching the (1 5 0) and (2 3 0) upper states are sometimes ambiguous as a consequence of strong anharmonic resonances with the (0 7 0) state. These features confirm the idea [6,8] that the vibrational states of HDO present unusually strong high-order resonance coupling due to large centrifugal distortion, and contradict in some way the opinion that monodeuterated water, HDO is a straightforward system with very limited vibrational perturbations [13].

Acknowledgments

We are indebted to A. Garnache (CEM2, Université de Montpellier) and A. Kachanov (Picarro, Sunnyvale, CA) for the development of ICLAS VECSEL in Grenoble and for providing the VECSEL samples. This work was supported by a collaborative project between CNRS and RFBR (PICS Grant 01-05-22002), as well as by the CNRS in the frame of the “Programme National de Chimie Atmosphérique” (PCNA). O.N. acknowledges the financial support from the Russian Foundation for Basic Researches (Grant Nos. 02-03-32512 and 02-07-90139). S. Hu (USTC, Hefei, China) is thanked for providing us the unpublished linelist of the HDO transitions measured by FT in [14].

References

- [1] H. Partridge, D.W. Schwenke, *J. Chem. Phys.* 106 (1997) 4618–4639.
- [2] D.W. Schwenke, H. Partridge, *J. Chem. Phys.* 113 (2000) 6592–6597.
- [3] P.F. Bernath, *Phys. Chem. Chem. Phys.* 4 (2002) 1501–1509.
- [4] J. Tennyson, N.F. Zobov, R. Williamson, O.L. Polyansky, P.F. Bernath, *J. Phys. Chem. Ref. Data* 30 (2001) 735–831.
- [5] T. Parekunnel, P.F. Bernath, N.F. Zobov, S.V. Shirin, O.L. Polyansky, J. Tennyson, *J. Mol. Spectrosc.* 210 (2001) 28–40.
- [6] O. Naumenko, E. Bertseva, A. Campargue, *J. Mol. Spectrosc.* 197 (1999) 122–132.
- [7] O. Naumenko, A. Campargue, *J. Mol. Spectrosc.* 199 (2000) 59–72.
- [8] O. Naumenko, E. Bertseva, A. Campargue, D. Schwenke, *J. Mol. Spectrosc.* 201 (2000) 297–309.
- [9] E. Bertseva, O. Naumenko, A. Campargue, *J. Mol. Spectrosc.* 203 (2000) 28–36.
- [10] A. Campargue, E. Bertseva, O. Naumenko, A. Campargue, *J. Mol. Spectrosc.* 204 (2000) 94–105.
- [11] S. Hu, H. Lin, S. He, J. Cheng, Q. Zhu, *Phys. Chem. Chem. Phys.* 1 (1999) 3727–3730.
- [12] A.D. Bykov, V.P. Lopasov, Yu.S. Makushkin, L.N. Sinitisa, O.N. Ulenikov, V.E. Zuev, *J. Mol. Spectrosc.* 94 (1982) 1–27.
- [13] A. Jenouvrier, M.F. Merienne, M. Carleer, R. Colin, A.-C. Vandaele, P.F. Bernath, O.L. Polyansky, J. Tennyson, *J. Mol. Spectrosc.* 209 (2001) 165–168.
- [14] Wang Xiang-Huai, He Sheng-Gui, Hu Shui-Ming, Zheng Jing-Jing, Zhu Qing-Shi, *Chin. Phys. Soc.* 9 (12) (2000) 885–891.
- [15] A. Garnache, A.A. Kachanov, F. Stoeckel, R. Houdré, *J. Opt. Soc. Am. B* 17 (2000) 1589–1598.
- [16] A. Garnache, A.A. Kachanov, F. Stoeckel, R. Planel, *Opt. Lett.* 24 (1999) 826–830.
- [17] E. Bertseva, A.A. Kachanov, A. Campargue, *Chem. Phys. Lett.* 351 (2002) 18–26.
- [18] Y. Ding, E. Bertseva, A. Campargue, *J. Mol. Spectrosc.* 212 (2002) 219–222.
- [19] Y. Ding, V. Perevalov, S.A. Tashkun, J.-L. Teffo, S. Hu, E. Bertseva, A. Campargue, *J. Mol. Spectrosc.* 220 (2003) 80–86.
- [20] Y. Ding, O. Naumenko, S. Hu, E. Bertseva, A. Campargue, *J. Mol. Spectrosc.* 220 (2003) 1–6.
- [21] E. Bertseva, A. Campargue, Y. Ding, A. Fayt, A. Garnache, J.S. Roberts, D. Romanini, *J. Mol. Spectrosc.* 219 (2003) 81–87.
- [22] L.S. Rothman, C.P. Rinsland, A. Goldman, S.T. Massie, D.P. Edwards, J.-M. Flaud, A. Perrin, C. Camy-Peyret, V. Dana, J.-Y. Mandin, J. Schroeder, A. McCann, R.R. Gamache, R.B. Wattson, K. Yoshino, K.V. Chance, K.W. Jucks, L.R. Brown, V. Nemtchinov, P. Varanasi, *J. Quant. Spectrosc. Radiat. Transfer* 60 (1998) 665–710.
- [23] J. Vander Auwera, R. El Hachtouki, L.R. Brown, *Mol. Phys.* 100 (2002) 3563–3576.
- [24] R. Toth, *J. Mol. Spectrosc.* 162 (1993) 20–40.
- [25] O.L. Polyansky, *J. Mol. Spectrosc.* 112 (1985) 79–87.
- [26] J.-M. Flaud, C. Camy-Peyret, A. Bykov, O. Naumenko, T. Petrova, A. Scherbakov, L.N. Sinitisa, *J. Mol. Spectrosc.* 183 (1997) 300–309.
- [27] B.P. Winnewisser, M. Winnewisser, O. Naumenko, unpublished results.
- [28] N. Papineau, C. Camy-Peyret, J.-M. Flaud, G. Guelachvili, *J. Mol. Spectrosc.* 92 (1982) 451–468.
- [29] O.N. Ulenikov, Shui-Ming Hu, E.S. Bekhtereva, G.A. Onopenko, Xiang-Huai Wang, Sheng-Gui He, Jing-Jing Zheng, Qing-Shi Zhu, *J. Mol. Spectrosc.* 208 (2001) 224–235.
- [30] T. Ohshima, H. Sasada, *J. Mol. Spectrosc.* 136 (1989) 250–263.